Biochemical and Biophysical Research Communications xxx (2018) 1–7

Contents lists available at ScienceDirect

Biochemical and Biophysical Research Communications

journal homepage: www.elsevier.com/locate/ybbrc

Sphingomyelin phosphodiesterase 1 (SMPD1) mediates the attenuation of myocardial infarction-induced cardiac fibrosis by astaxanthin

Yu Shi [a, 1], Peng Lin [b, 1], Xiaoning Wang [a], Guangmei Zou [c, **], Kefeng Li [d, *]

[a] Department of Cardiology, Yantai Yuhuangding Hospital, Yantai, Shandong Province, 264001, China
[b] Department of Critical Care Medicine, Yantai Yuhuangding Hospital, Yantai, Shandong Province, 264001, China
[c] Department of Cardiac Surgery ICU, Yantai Yuhuangding Hospital, Yantai, Shandong Province, 264001, China
[d] School of Medicine, University of California, San Diego, San Diego, CA, 92103, USA

ARTICLE INFO

Article history:
Received 1 June 2018
Accepted 11 June 2018
Available online xxx

Keywords:
Cardiac fibrosis
Myocardial infarction
Astaxanthin
Lipidomics
SMPD1

ABSTRACT

Uncontrolled cardiac fibrosis following myocardial infarction (MI) is a critical pathological change leading to heart failure. Current pharmacotherapies are limited by unsatisfactory efficacy and undesired systemic side effects. Astaxanthin (ASX) is a natural carotenoid with strong antioxidant and anti-inflammatory activities. The effects of ASX on MI-induced cardiac fibrosis and the underlying mechanisms remain largely unknown. In this study, after the establishment of MI model, mice were administrated with ASX (200 mg/kg•d) for 4 weeks. We found that ASX treatment attenuated cardiac fibrosis and improved heart function following MI, as evidenced by reduced collagen I/III ratio, hydroxyproline content and left ventricular end diastolic pressure (LVEDP). Lipidomic analysis revealed the overaccumulation of myocardial ceramides in mice with cardiac fibrosis, which was normalized by ASX treatment. Molecular docking analysis showed that ASX produced a tight fit in the pocket of sphingomyelin phosphodiesterase 1 (SMPD1), a key enzyme in the production of ceramides. Western blot analysis confirmed the significant inhibition of SMPD1 expression by ASX. Furthermore, MI-induced overexpression of transforming growth factor β1 (TGF-β1) and phosphorylated SMAD2/3 were attenuated by ASX administration. SMPD1 knockout (KO) abrogated the beneficial effect of ASX. Taken together, our results suggest that the cardioprotective effects of ASX are mediated by SMPD1 through the indirection inhibition of TGF- β1/SMAD signaling cascade.

1. Introduction

Cardiac fibrosis refers to the excessive and disorganized deposition of myocardial collagens in response chronic insult to the myocardium such as myocardial infarction (MI) [1]. Uncontrolled fibrosis in the heart leads to fibrotic scar formation, wall stiffness, impairment of cardiac function and eventually to heart failure (HF) [2]. The process of fibrogenesis is primarily orchestrated by members of transforming growth factor (TGF)-β [3]. It was reported that overexpression of TGF- β isoform TGF-β1 in the mouse heart induces cardiac fibrosis [4].

Currently, there is lack of effective treatment for cardiac fibrosis. Interventions directly targeting TGF-β including TGF-β1 specific antibody and TGF-β1 kinase inhibitors either produce undesired systemic side effects or show no improvement due to the versatile physiological functions of TGF-β [5]. Inhibition of TGF-β downstream signaling pathways is proposed to be a better treatment strategy for fibrotic disorders [6]. TGF-β induces cardiac fibrosis via the activation of either canonical Smad signaling [7] or non-canonical signaling pathways such as PI3K/AKT and ERK/MAPK [8,9].

Ceramides, a class of sphingolipids, are not only the essential structural components of cell membranes but also function as second messenger molecules in cell signaling and inflammation [10]. Increasing evidence supports the direct role of ceramide signaling in cardiovascular diseases [11]. For instance, ceramides have been linked with processes involved in the atherosclerotic

* Corresponding author.
** Corresponding author.
E-mail addresses: zouguangmei2006@126.com (G. Zou), kli@ucsd.edu (K. Li).
[1] Y.S and P.L contributed equally to this work.

https://doi.org/10.1016/j.bbrc.2018.06.054
0006-291X/

development and cardiac remodeling and dysfunction [12]. Our previous also showed that increased plasma ceramides level might be used for the prediction of restenosis after percutaneous coronary intervention (PCI) [13]. Sphingomyelin phosphodiesterase 1 (SMPD1) is the key enzyme that coverts sphingomyelins (SMs) to the proinflammatory and proapoptotic second messenger ceramides [14]. SMPD1 is best known for its involvement in regulating immune cell functions and Niemann-Pick disease (NPD) [15]. However, the role of SMPD1 in the pathogenesis of cardiac fibrosis remained uncertain.

Astaxanthin (ASX) is a natural carotenoid and has been approved by US FDA as a food additive and dietary supplement [16]. In vitro and in vivo studies of ASX showed strong antioxidant and anti-inflammatory activities [17,18]. ASX has been shown to alleviate pulmonary, peritoneal and liver fibrosis through various tissue-specific mechanisms such as modulating autophagy and promoting apoptosis [19,20]. However, little information is available about its effect on cardiac fibrosis. The effect ASX on myocardial fibrosis following MI has not been reported yet. A recent study reported that ASX attenuated pressure overload-induced cardiac dysfunction and myocardial fibrosis partially by the activation of SIRT1 [21]. However, SIRT1 is a nuclear protein that mainly localized in the nucleus [22]. In contrast, ASX generally interacts with proteins on the plasma membrane due to its unique molecular structure [23]. The chance of the direct interaction between ASX and SIRT1 is fairly low. The mechanisms of action of ASX are still incompletely understood.

In this study, we investigated the effect of ASX on cardiac fibrosis after MI in mice. We aimed to elucidate the mechanisms of action of ASX using a comprehensive and unbiased lipidomic approach. The identified biological target of ASX was further validated by computational docking, western blot analysis and in vivo knockout tests. Our study highlighted the role of SMPD1 in the mediation of the attenuation of MI-induced cardiac fibrosis by ASX. The changes of TGF-β1 and the downstream signaling pathways in response to ASX treatment were also studied.

2. Experimental methods

2.1. Animals

Male C57BL/6 J mice (wild type, 8-week-old, 20–22 g) were obtained from the Experimental Animal Center of Shandong University. Smpd1 knockout mice (Smpd1$^{-/-}$, 8-week-old) were purchased from Nanjing Biomedical Research Institute of Nanjing University. All the animal protocols in this study were approved by Institutional Animal Care and Use Committee of Yantai Yuhuangding Hospital (YTYHD-2016-3218) and carried out in accordance with the National Institutes of Health (NIH) Guidelines for the use of animals in research.

2.2. Mice model of myocardial infarction (MI)

The mice model of MI was performed by the ligation of the left anterior descending artery (LAD) as described [24]. Briefly, mice were anesthetized with 2% isofluorane. The hearts were exposed and an 8-0 Prolene suture (Ethicon, Norderstedt, Germany) was used to ligate the LAD proximal with one single suture. The LAD position was at a site about 2–3 mm from LAD origin. The sham group underwent the same thoracotomy procedure except for LAD ligation.

2.3. Administration of astaxanthin (ASX)

ASX was purchased from Jingzhou Natural Astaxanthin Co. Ltd. (Jingzhou, China), dissolved in DMSO and diluted in 0.9% saline. The mice were randomly divided into three groups: (1) MI + ASX (Wild type with MI and treated with ASX), (2) MI + vehicle (Wild type, MI and 0.9% saline) (3) Sham + vehicle (Wild type with sham surgery and treated with 0.9% saline). Mice in ASX treated groups were administered with 200 mg/kg body weight of ASX daily for 4 weeks via oral gavage. Equal amount of 0.9% saline solution was given as vehicle treated groups. Eight mice were set up for each group.

2.4. Determination of hemodynamic parameters

Hemodynamic parameters including systolic blood pressure (SBP), diastolic blood pressure (DBP), left ventricular systolic pressure (LVSP), left ventricular end diastolic pressure (LVEDP), $+dp/dt_{max}$, $-dp/dt_{min}$ were measured after 4 weeks of treatment using a Millar pressure catheter. Mice were then sacrificed and the hearts were removed, weighed and stored at −80 °C for further analysis.

2.5. Quantification of myocardial hydroxyproline (Hyp)

The analysis of Hyp in mice heart tissue was conducted as described by a previous protocol [25]. Briefly, the samples were washed with saline and hydrolyzed with 6 mol/l HCl at 100 °C for overnight. The Hyp content was determined by the addition of *p*-dimethylaminobenzaldehyde and quantified on a Multiplate Spectrometer at 560 nm. The amount of Hyp in the issue was expressed as μg/g of fresh tissue. Measurements of each group were performed in triplicate, and the standard deviation was less than ±10%.

2.6. Immunohistochemical staining of collagen I and III

Immunohistochemistry was performed using DAKO EnVision^{+} detection kit (DakoCytomation, USA) according to the manufacturer's instructions. Primary antibodies against type I collagen (Abcam, USA) and type III collagen (Abcam, USA) were used. A positive reaction was observed as brown staining. The area of positive immunostaining was quantified using a computer image analysis system (Image Pro Plus 6.0). The ratio of type I/III collagen was calculated.

2.7. Lipidomic analysis of heart tissues

Lipidomic profiling was conducted as before with slight modifications [26]. Briefly, the lipids were extracted from 50 mg of frozen heart tissues using 1.5 mL of prechilled extraction buffer containing methanol-acetonitrile-acetone-water (30:30:30:10, v/v/v). The mixture was centrifuged at 16,000 g for 10 min and the supernatant was taken for lipidomic profiling using LC-MS/MS. Lipid analysis was conducted using a UHPLC 1260 system (Agilent, USA) coupled with a Qtrap 4500 mass spectrometer (SCIEX, USA) operated in multiple reaction monitoring (MRM) mode. The lipids were separated on an ACQUITY UPLC BEH C_{18} column (2.1 × 150 mm, 1.7 μm). Mobile phase A was 95% H_2O with 20 mM NH4HCOOH and 5% ACN (pH 4). Mobile phase. B was 100% acetonitrile. The flow rate was 300 μl/min. All major lipids classes in mice hearts were targeted.

2.8. Molecular docking analysis

Docking analysis between ASX and sphingomyelin phosphodiesterase 1 (SMPD1) protein was conducted using SwissDock (http://www.swissdock.ch/). The PDB code for SMPD1 was 5FIB and the zinc accession no. for ASX was 17653967. The data visualization and analysis were performed using Chimera 1.12.

Please cite this article in press as: Y. Shi, et al., Sphingomyelin phosphodiesterase 1 (SMPD1) mediates the attenuation of myocardial infarction-induced cardiac fibrosis by astaxanthin, Biochemical and Biophysical Research Communications (2018), https://doi.org/10.1016/j.bbrc.2018.06.054

2.9. Western blot analysis

Total protein was extracted from left ventricular myocardial tissues and the concentration was quantified using a Pierce BCA assay kit (ThermoFisher, USA). The protein lysates (30–50 μg protein) were separated by 6%–12% SDS-PAGE. Primary antibodies including anti-*p*-Smad2/3 (1:1000, R&D Systems, USA), anti-Smad2/3 (1:1000, Cell Signaling Technology, USA) and anti-GAPDH (1:1000 dilution, Cell Signaling Technology) were used. After incubation with HRP-conjugated secondary antibodies (1:500; Santa Cruz Biotechnology, USA), the protein bands were visualized using a SuperSignal ECL kit (Thermo, USA) and detected using a chemiluminescence reader (Image Quant LAS4000 mini, GE, USA). Protein levels were analyzed using Image J software and normalized to the corresponding GAPDH levels. The experiments were repeated 3 times.

2.10. Quantitative real-time PCR analysis of TGF-β1 expression

Total RNA was extracted from heart tissue samples using the TRIzol reagent (Invitrogen, USA). The mRNA expression of *TGF-β1* and GAPDH was detected using a 7500 Real-Time PCR Systems (Applied Biosystems, USA). The expression level of *TGF-β1* was normalized to that of the housekeeping gene GAPDH in the same tissue.

2.11. $Smpd1^{-/-}$ knockout

To validate the role of SMPD1, knockout (KO) mice ($Smpd1^{-/-}$) underwent the same MI procedure and ASX treatment (200 mg/kg body weight for 4 weeks) as described above for the wild type animals. Four groups were set up: (1) KO + MI + ASX (KO mice with MI and ASX), (2) KO + MI + vehicle (KO mice with MI and 0.9% saline) (3) KO + sham + vehicle (KO mice with sham surgery and 0.9% saline). (4) Wild type + MI + vehicle (Wild type mice with MI and 0.9% saline). Six replicates were used for each group. Total ceramide was measured by LC-MS/MS according to the published method [27]. Other measurements were same as described above.

2.12. Statistical analysis

Data were expressed as mean ± standard deviation (SD). Statistical analysis was conducted using GraphPad Prism 7.0 (Prism, USA). Differences were determined using student's t-test or one-way ANOVA. A p-value of 0.05 was considered as significantly different.

3. Results

3.1. ASX attenuated the cardiac dysfunction after MI

To explore the effect of ASX in protecting cardiac function after MI, we examined the changes of hemodynamic parameters. As showed in Table 1, the cardiac dysfunction was observed in MI + vehicle mice as evidenced by the increased values of SBP, DBP, LVSP and ± dp/dt and the decreased LVEDP compared with the sham group. However, ASX treatment improved mice heart function by lowering the values of SBP, DBP, LVSP and ± dp/dt and increasing LVEDP compared with MI + vehicle (All $p < 0.05$, Table 1).

Table 1
The improvement of hemodynamic parameters after 4 weeks of ASX treatment.

Parameters	Sham + vehicle	MI + vehicle	MI + ASX
SBP (mmHg)	129.1 ± 3.4	$105.8 \pm 2.1^{\Delta}$	$116.7 \pm 4.2^{\Delta *}$
DBP (mmHg)	104.0 ± 3.2	$77.1 \pm 2.9^{\Delta}$	$85.9 \pm 1.3^{\Delta *}$
LVSP (mmHg)	135.4 ± 27.3	$104.1 \pm 11.3^{\Delta}$	$123.9 \pm 12.7^{*}$
LVEDP (mmHg)	2.2 ± 0.4	$9.6 \pm 1.2^{\Delta}$	$5.1 \pm 2.6^{\Delta *}$
+dp/dt (mmHg/s)	6316 ± 212	$3338 \pm 182^{\Delta}$	$4914 \pm 111^{\Delta *}$
-dp/dt (mmHg/s)	6019 ± 224	$3053 \pm 336^{\Delta}$	$4535 \pm 340^{\Delta *}$

Data are mean ± SD (n = 8 per group); *$p < 0.05$ compared to MI model group treated with saline and $\Delta p < 0.05$ compared with sham group.

3.2. ASX alleviated MI-induced cardiac fibrosis

To assess the effect of ASX on MI-induced cardiac fibrosis, we analyzed the expression of collagen I and collagen III. Compared with the sham group, excessive collagen especially collagen type I was observed in MI + vehicle group (Fig. 1A). ASX treatment reduced the accumulation of collagen indicating the alleviation of cardiac fibrosis (Fig. 1A). We also examined the change of collagen type I/III ratio in the non-infarcted zone of mice hearts. The ratio in MI + vehicle was significantly higher than that in the sham group ($p < 0.01$, Fig. 1B). The collagen type I/III ratio dramatically decreased in response to ASX treatment compared with MI + vehicle. In addition, hydroxyproline content, a sensitive biochemical marker indicating collagen fiber changes, increased following MI ($p < 0.01$, Fig. 1C). However, it was substantially reduced by ASX treatment ($p < 0.05$, Fig. 1C).

3.3. ASX reduced the increased level of myocardial ceramide-induced by MI

To explore the mechanisms of ASX on the alleviation of cardiac fibrosis, we performed the broad-spectrum lipidomic analysis of the heart tissue samples. Lipidomics followed by PLS-DA revealed the distinct metabolic differences between the model and sham group as the complete separation of two groups (Fig. 2A). ASX treatment (MI + ASX) drove the metabolism of MI animals (MI + vehicle) strongly in the direction of Sham + vehicle group (Fig. 2A). Variable importance in projection (VIP) analysis showed the most discriminating metabolites between three groups (Fig. 2B). Surprisingly, the top 7 metabolites were ceramides (Cer) and sphingomyelins (SMs). For example, MI and cardiac fibrosis led to the accumulation of Cer(d18:1/18:0), Cer(d18:1/16:1) and Cer(d18:1/18:1) in MI + vehicle group compared with the sham + vehicle group. The concentration of Cer dramatically decreased after ASX treatment. In contrast, SM(d18:1/24:2) was significantly lower in MI + vehicle than the sham group (Fig. 2B). ASX treatment increased SM(d18:1/24:2) in MI + ASX group. Lipidomic analysis indicated that ASX might alleviate cardiac fibrosis through targeting on ceramide metabolism.

3.4. ASX inhibited the expression of SMPD1

The hydrolysis of SMs through SMPD1 is the major route for ceramides production in the heart. To investigate the effect of ASX on SMPD1, we first conducted the computational docking analysis of SMPD1-ASX interaction. ASX produced a tight fit in the pocket of SMPD1 with the free binding energy of −180.2 kcal/mol (Fig. 2C). We next the expression of SMPD1 in the heart tissues. We found that compared to the sham + vehicle group, SMPD1 was significantly upregulated MI + vehicle ($p < 0.01$) (Fig. 2D). However, ASX treatment led to a dramatic inhibition of SMPD1 expression, which was consistent with the decrease of ceramide level in heart tissues (Fig. 2D).

Please cite this article in press as: Y. Shi, et al., Sphingomyelin phosphodiesterase 1 (SMPD1) mediates the attenuation of myocardial infarction-induced cardiac fibrosis by astaxanthin, Biochemical and Biophysical Research Communications (2018), https://doi.org/10.1016/j.bbrc.2018.06.054

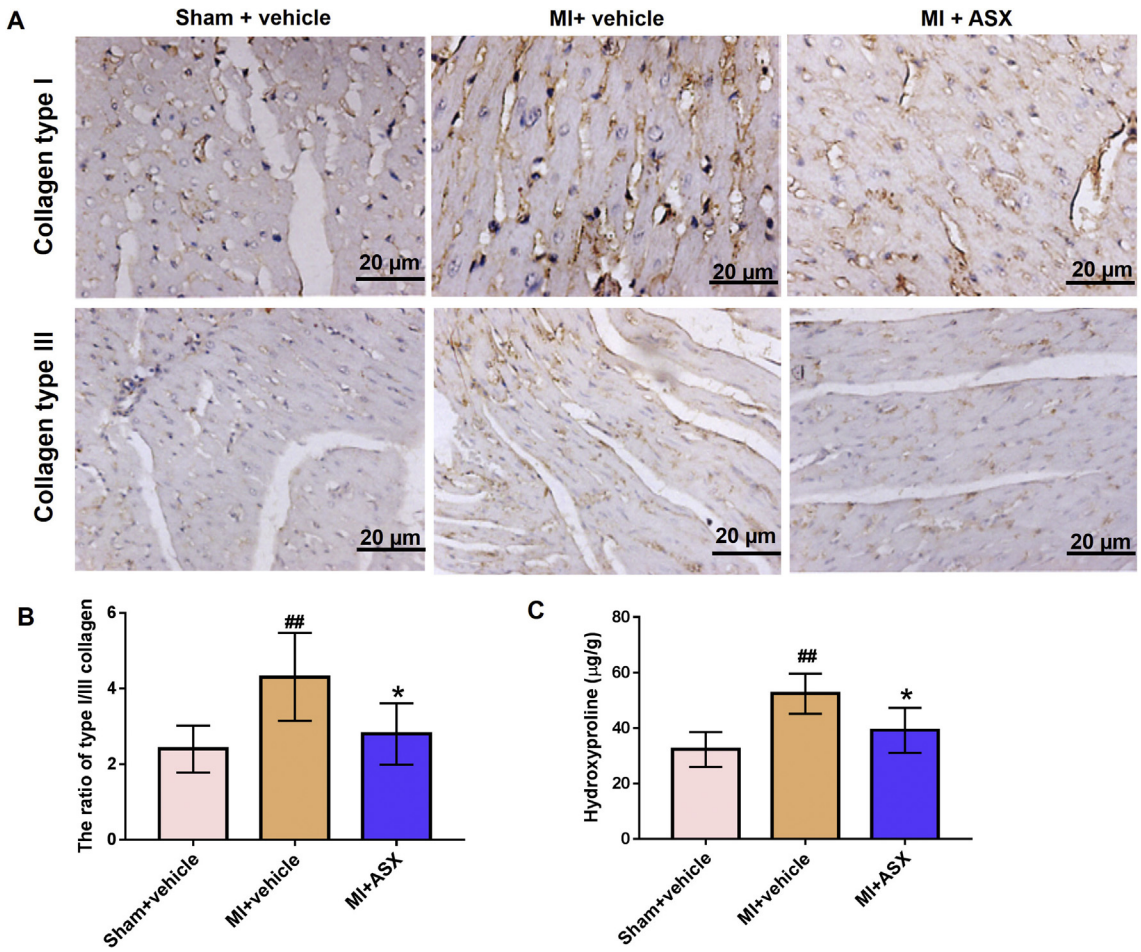

Fig. 1. Effect of ASX treatment on MI-induced cardiac fibrosis. (A) Immunohistochemical staining for collagen type I and III. Brown particles around the cells indicated the expression of collagen protein. Magnification: X400. (B) The changes of the ratio of type I/III collagen after ASX treatment. Data were mean ± SD. n = 6 per group. (C) The content of hydroxyproline in mice hearts. Data were mean ± SD. n = 3 per group. ##p < 0.01 vs sham + vehicle and *p < 0.05 vs MI + vehicle. (For interpretation of the references to colour in this figure legend, the reader is referred to the Web version of this article.)

3.5. ASX inhibited TGF-β1-Smad2/3 signaling pathway

Because of the essential role of TGF-β1 in cardiac fibrosis, we next investigated TGF-β1 expression in heart tissues. As shown in Fig. 3A, the mRNA level of TGF-β1 was significantly elevated in MI + vehicle compared with the sham group ($p < 0.01$). ASX treatment induced the dramatic downregulation of TGF-β1 compared with MI + vehicle.

We next explored whether TGF-β1- Smad2/3 signaling pathway was altered by ASX treatment. Western blot analysis was performed to detect the phosphorylation of Smad2/3. We found that Smad2/3 phosphorylation was obviously higher in MI + vehicle group. ASX treatment led to the significant reduction of Smad2/3 phosphorylation (Fig. 3B and C). The PI3K/AKT and ERK/MAPK signaling pathways were also explored and no significant difference was observed after ASX treatment ($p > 0.05$, Data was not shown).

3.6. Knockout (KO) of SMPD1 alleviated cardiac fibrosis and abolished the drug effect of ASX

To validate the role of SMPD1 in the mediation of ASX drug effect, SMPD1 KO mice were generated and compared with the wild type. Total ceramides in heart tissues of KO mice showed a significant decrease compared with wild type mice, which indicated the success of the knockout model (Wild + MI + vehicle vs KO + MI + vehicle, $p < 0.01$, Fig. 4A). There was no dramatic difference in cardiac ceramides level between infracted KO mice with and without ASX treatment (KO + MI + vehicle vs KO + MI + ASX, $p = 0.841$) (Fig. 4A). Compared with wild type, KO mice showed significantly less impairment in LVEDP following MI (Wild + MI + vehicle vs KO + MI + vehicle, $p < 0.01$) (Fig. 4B). However, ASX treatment did not lead to the reduction of LVEDP in KO mice as it did in wild type following MI (KO + MI + vehicle vs KO + MI + ASX, $p = 0.991$) (Fig. 4B). KO mice treated with ASX showed no significant difference in cardiac hydroxyproline content from the MI model group following MI (KO + MI + ASX vs KO + MI + vehicle, $p = 0.854$) (Fig. 4C). In addition, Smpd1 knockout led to the dramatic reduction of type I/type III collagen ratio compared with the wild type mice with MI (Wild + MI + vehicle vs KO + MI + vehicle, $p < 0.05$) (Fig. 4D). In contrast, ASX treatment in KO mice with MI did not further decrease the ratio of type I/type III collagen in mice heart tissue (KO + MI + vehicle vs KO + MI + ASX, $p = 0.732$) (Fig. 4D).

Based on the above fact, we proposed that the action of ASX on the attenuation of cardiac fibrosis might be through the direct inhibition of SMPD1, which then indirectly resulted in the inhibition of TGF-β1-Smad2/3 signaling pathway (Fig. 4E).

Please cite this article in press as: Y. Shi, et al., Sphingomyelin phosphodiesterase 1 (SMPD1) mediates the attenuation of myocardial infarction-induced cardiac fibrosis by astaxanthin, Biochemical and Biophysical Research Communications (2018), https://doi.org/10.1016/j.bbrc.2018.06.054

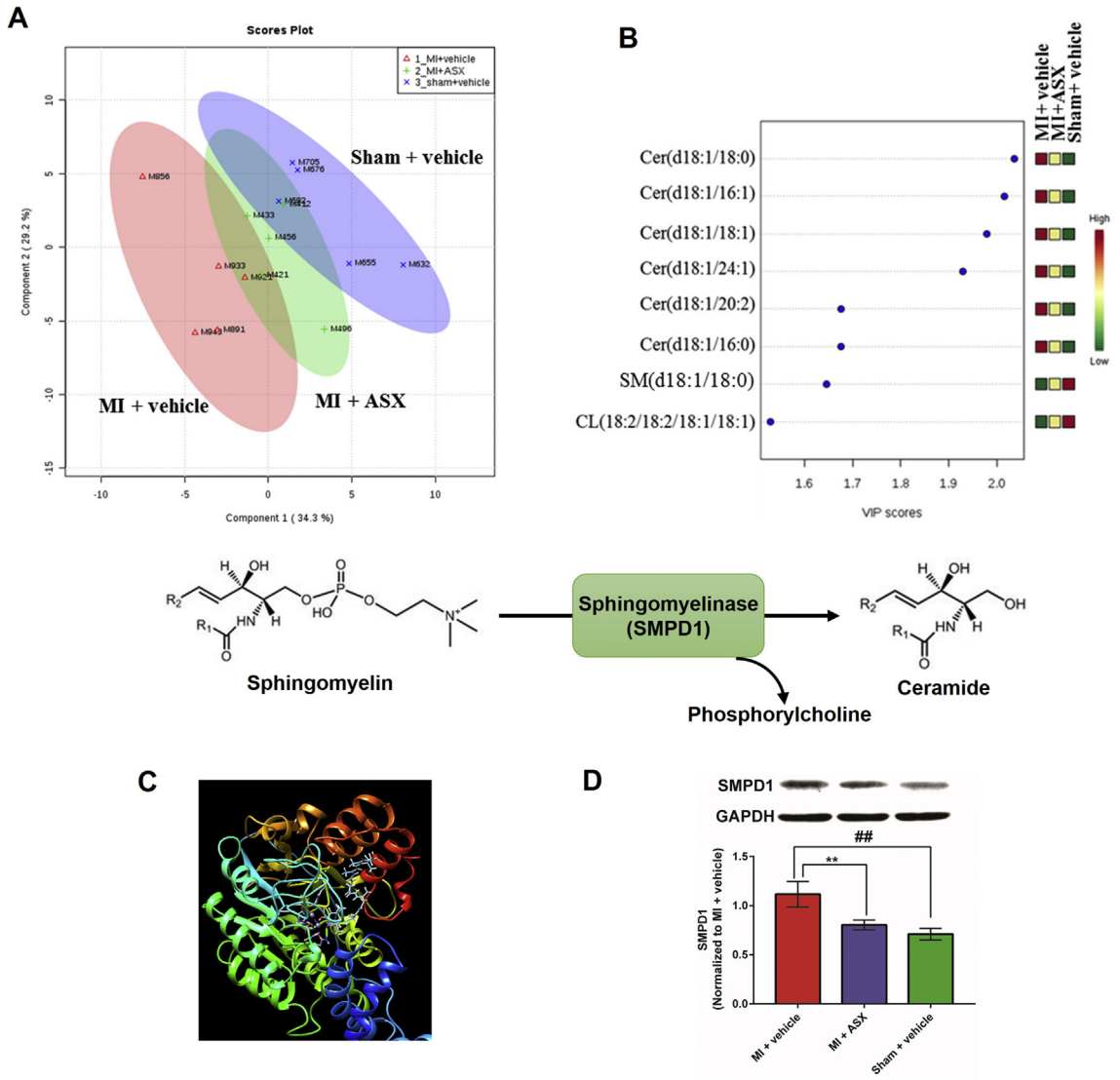

Fig. 2. ASX inhibited the expression of SMPD1. (A) PLS-DA showed the dramatic differences in lipids metabolism between MI and sham group. Treated with ASX drove the lipid metabolism towards the sham group. N = 6 mice per group. (B) VIP analysis showed the top differential lipids between the groups. (C) Molecular docking analysis showed the low-energy binding of SMPD1 protein and ASX ligand. SMPD1 protein was depicted in ribbon representation and the ligand ASX was displayed in the ball and stick representation. (D) ASX inhibited the upregulation of SMPD1 expression induced by MI in mice hearts. GADPH is the loading control. The relative expression was mean ± SD (n = 3 independent experiments). **p < 0.01 vs MI + vehicle group, ##p < 0.01 vs sham + vehicle.

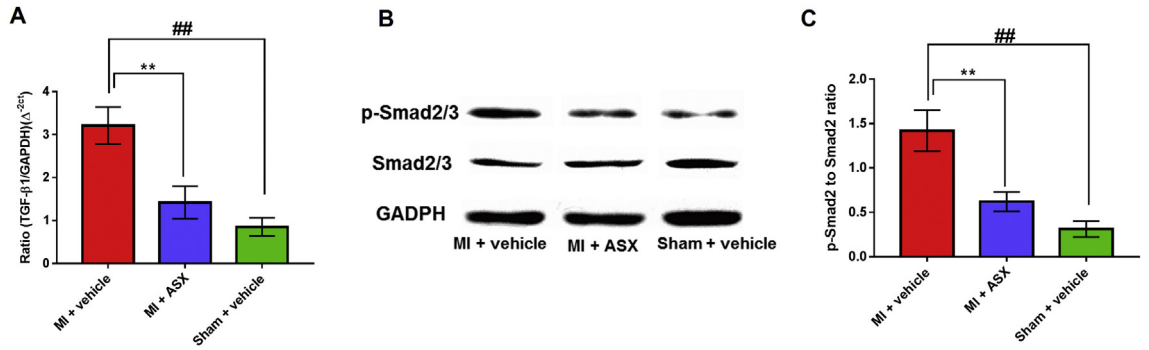

Fig. 3. ASX inhibited the expression of TFG-β1 and its downstream signaling pathway in heart tissues. (A) TGF-β1 expression was significantly downregulated in heart tissues after ASX treatment. **p < 0.01 vs MI + vehicle group, ##p < 0.01 vs sham + vehicle. (B) The representative western blot image of *p*-Smad2/3 and Smad2/3 levels in heart tissue. (C) ASX inhibited the MI-induced phosphorylation of Smad2/3. Data were mean ± SD (n = 3 independent experiments). **p < 0.01 vs MI + vehicle group, ##p < 0.01 vs sham + vehicle.

Please cite this article in press as: Y. Shi, et al., Sphingomyelin phosphodiesterase 1 (SMPD1) mediates the attenuation of myocardial infarction-induced cardiac fibrosis by astaxanthin, Biochemical and Biophysical Research Communications (2018), https://doi.org/10.1016/j.bbrc.2018.06.054

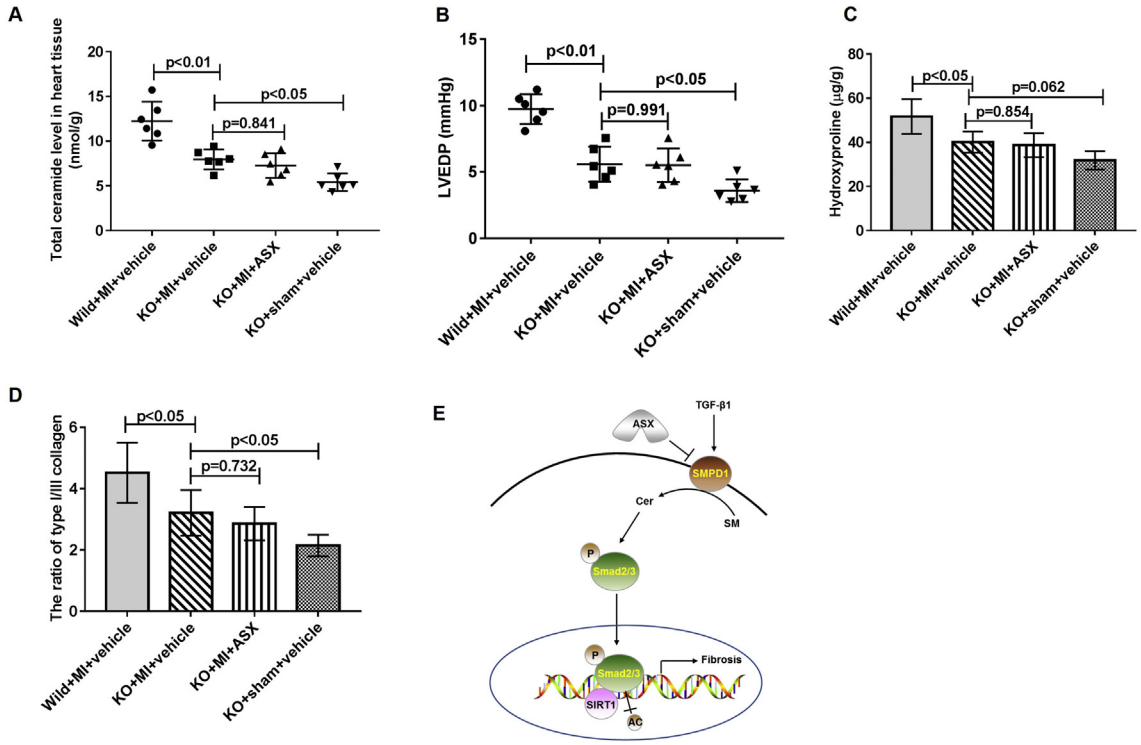

Fig. 4. Knockout (KO) of SMPD1 abolished the drug effect of ASX treatment. (A) Total ceramides level was significantly lower in KO mice compared with the wild type following MI ($p < 0.01$). (B) No significant difference was found for LVEDP between post-MI KO mice treated with vehicle and ASX ($p = 0.991$). (C) ASX treatment did not decrease the MI-induced hydroxyproline accumulation in KO mice (D) The type I/III collagen ratio was not reduced after ASX treatment in KO mice following MI. Data were mean ± SD ($n = 6$ mice per group). (E) The schematic diagram of the mechanisms of action of ASX on the attenuation of cardiac fibrosis.

4. Discussion

Cardiac fibrosis is a critical pathological change towards the development of heart failure caused by MI. Although several anti-fibrotic drugs have been available in the market, there is an urgent need for new treatment strategies due to the limited efficacy and unsatisfactory safety side effects of current therapies. In this study, we discovered for the first time that ASX treatment alleviated myocardial fibrosis, suppressed the ventricular remodeling and improved the cardiac function after MI. Consistent with our findings, a recent study demonstrated the protective effects of ASX on cardiac tissues in isoproterenol-administered rats [28].

Our lipidomic analysis revealed the upregulation of ceramide metabolism in mice heart tissues following MI. The accumulation of ceramides had also been observed during ischemia and reperfusion in animal models of heart failure, and in human cardiomyopathies [29]. In addition, the level of total ceramides was reported to be associated with liver fibrosis [30].

Ceramides are synthesized by two major pathways: *de novo* synthesis pathway through SPT and the hydrolysis of SMs through SMPD1. The later route produces about 70% of total cellular ceramides in the heart due to the presence of triglyceride-rich (TG-rich) lipoproteins [31]. We, therefore, hypothesized that the reduction of ceramides after ASX treatment was caused by the inhibition of SMPD1, which was validated by subsequent western blot analysis, molecular docking analysis and SMPD1 knockout in vivo test.

Our current study showed that targeting SMPD1 by ASX might be a better treatment strategy for cardiac fibrosis. SMPD1 inhibition has also been showed to normalize depression-like behaviors [32], attenuate lung inflammation [33] and prevent acellular capillary formation [14]. In addition, a previous study showed that overexpression of SMPD1 promotes liver fibrosis [34].

A notable finding in our study is the identification of the role of SMPD1 in the mediation of the anti-fibrotic effect of ASX. Zhang et al. reported that SIRT1 is involved in the attenuation of fibrosis by ASX [21]. We further showed that SMPD1 is required for ASX's functions and knockout of SMPD1 abolishes the beneficial effect of ASX. TGF-β1 and its downstream signaling cascades including Smad2/3/SIRT1 and AT1R/p38MAPK are known to play essential roles in the pathogenesis of cardiac fibrosis [35]. We found that ASX inhibits both TGF-β and Smad2/3. No significant inhibitory effect was observed for AT1R/p38 MAPK pathway. The “cross-talk” between ceramide metabolism, Smpd1, and TGF-β1/Smad signaling are largely unknown. A recent report showed that the increase of ceramide promotes TGF-β1/Smad signaling in the skin [36].

In summary, our study showed that ASX treatment suppresses cardiac fibrosis and improves heart function after MI. The protective effects of ASX are mediated by SMPD1. Knockout of Smpd1 diminishes the effects of ASX. ASX inhibits Smpd1 and decreases ceramide metabolism, which then alleviates cardiac fibrosis through the indirect reduction of TGF-β1/Smad signaling.

Conflicts of interest

The authors declare no conflict of interest.

Acknowledgments

None.

References

[1] M. Gyongyosi, J. Winkler, I. Ramos, et al., Myocardial fibrosis: biomedical research from bench to bedside, Eur. J. Heart Fail. 19 (2017) 177–191.

Please cite this article in press as: Y. Shi, et al., Sphingomyelin phosphodiesterase 1 (SMPD1) mediates the attenuation of myocardial infarction-induced cardiac fibrosis by astaxanthin, Biochemical and Biophysical Research Communications (2018), https://doi.org/10.1016/j.bbrc.2018.06.054

[2] V. Talman, H. Ruskoaho, Cardiac fibrosis in myocardial infarction-from repair and remodeling to regeneration, Cell Tissue Res. 365 (2016) 563–581.
[3] X.M. Meng, D.J. Nikolic-Paterson, H.Y. Lan, TGF-beta: the master regulator of fibrosis, Nat. Rev. Nephrol. 12 (2016) 325–338.
[4] M. Dobaczewski, W. Chen, N.G. Frangogiannis, Transforming growth factor (TGF)-beta signaling in cardiac remodeling, J. Mol. Cell. Cardiol. 51 (2011) 600–606.
[5] F. Jiang, G.S. Liu, G.J. Dusting, E.C. Chan, NADPH oxidase-dependent redox signaling in TGF-beta-mediated fibrotic responses, Redox Biol. 2 (2014) 267–272.
[6] A. Biernacka, M. Dobaczewski, N.G. Frangogiannis, TGF-beta signaling in fibrosis, Growth Factors 29 (2011) 196–202.
[7] K.L. Walton, K.E. Johnson, C.A. Harrison, Targeting TGF-beta mediated SMAD signaling for the prevention of fibrosis, Front. Pharmacol. 8 (2017) 461.
[8] S. Zhang, R. Cui, The targeted regulation of miR-26a on PTEN-PI3K/AKT signaling pathway in myocardial fibrosis after myocardial infarction, Eur. Rev. Med. Pharmacol. Sci. 22 (2018) 523–531.
[9] W. Zhong, W.F. Shen, B.F. Ning, et al., Inhibition of extracellular signal-regulated kinase 1 by adenovirus mediated small interfering RNA attenuates hepatic fibrosis in rats, Hepatology 50 (2009) 1524–1536.
[10] X. He, E.H. Schuchman, Ceramide and ischemia/reperfusion injury, J. Lipids 2018 (2018) 3646725.
[11] K. Huynh, Coronary artery disease: ceramides predict CV death in stable CAD and ACS, Nat. Rev. Cardiol. 13 (2016) 381.
[12] R. Ji, H. Akashi, K. Drosatos, et al., Increased de novo ceramide synthesis and accumulation in failing myocardium, JCI Insight 2 (2017).
[13] S. Cui, K. Li, L. Ang, et al., Plasma phospholipids and sphingolipids identify stent restenosis after percutaneous coronary intervention, JACC Cardiovasc. Interv. 10 (2017) 1307–1316.
[14] M. Opreanu, M. Tikhonenko, S. Bozack, et al., The unconventional role of acid sphingomyelinase in regulation of retinal microangiopathy in diabetic human and animal models, Diabetes 60 (2011) 2370–2378.
[15] E.H. Schuchman, Acid sphingomyelinase, cell membranes and human disease: lessons from Niemann-Pick disease, FEBS Lett. 584 (2010) 1895–1900.
[16] M. Guerin, M.E. Huntley, M. Olaizola, Haematococcus astaxanthin: applications for human health and nutrition, Trends Biotechnol. 21 (2003) 210–216.
[17] T. Niu, R. Xuan, L. Jiang, et al., Astaxanthin induces the Nrf2/HO-1 antioxidant pathway in human umbilical vein endothelial cells by generating trace amounts of ROS, J. Agric. Food Chem. 66 (2018) 1551–1559.
[18] M. Zuluaga, V. Gueguen, D. Letourneur, G. Pavon-Djavid, Astaxanthin-antioxidant impact on excessive reactive oxygen species generation induced by ischemia and reperfusion injury, Chem. Biol. Interact. 279 (2018) 145–158.
[19] J. Zhang, P. Xu, Y. Wang, et al., Astaxanthin prevents pulmonary fibrosis by promoting myofibroblast apoptosis dependent on Drp1-mediated mitochondrial fission, J. Cell Mol. Med. 19 (2015) 2215–2231.
[20] M. Shen, K. Chen, J. Lu, et al., Protective effect of astaxanthin on liver fibrosis through modulation of TGF-beta1 expression and autophagy, Mediat. Inflamm. 2014 (2014) 954502.
[21] J. Zhang, Q.Z. Wang, S.H. Zhao, et al., Astaxanthin attenuated pressure overload-induced cardiac dysfunction and myocardial fibrosis: partially by activating SIRT1, Biochim. Biophys. Acta 1861 (2017) 1715–1728.
[22] V. Byles, L.K. Chmilewski, J. Wang, L. Zhu, L.W. Forman, D.V. Faller, Y. Dai, Aberrant cytoplasm localization and protein stability of SIRT1 is regulated by PI3K/IGF-1R signaling in human cancer cells, Int. J. Biol. Sci. 6 (2010) 599–612.
[23] E. Reszczynska, R. Welc, W. Grudzinski, et al., Carotenoid binding to proteins: modeling pigment transport to lipid membranes, Arch. Biochem. Biophys. 584 (2015) 125–133.
[24] J.N. Andrade, J. Tang, M.T. Hensley, et al., Rapid and efficient production of coronary artery ligation and myocardial infarction in mice using surgical clips, PLoS One 10 (2015) e0143221.
[25] B. Qiu, F. Wei, X. Sun, et al., Measurement of hydroxyproline in collagen with three different methods, Mol. Med. Rep. 10 (2014) 1157–1163.
[26] L. Lin, B. Cao, Z. Xu, et al., In vivo HMRS and lipidomic profiling reveals comprehensive changes of hippocampal metabolism during aging in mice, Biochem. Biophys. Res. Commun. 470 (2016) 9–14.
[27] T. Kasumov, H. Huang, Y.M. Chung, et al., Quantification of ceramide species in biological samples by liquid chromatography electrospray ionization tandem mass spectrometry, Anal. Biochem. 401 (2010) 154–161.
[28] M.N. Alam, M.M. Hossain, M.M. Rahman, et al., Astaxanthin prevented oxidative stress in heart and kidneys of isoproterenol-administered aged rats, J. Diet. Suppl. 15 (2018) 42–54.
[29] A. Chokshi, K. Drosatos, F.H. Cheema, et al., Ventricular assist device implantation corrects myocardial lipotoxicity, reverses insulin resistance, and normalizes cardiac metabolism in patients with advanced heart failure, Circulation 125 (2012) 2844–2853.
[30] G. Grammatikos, N. Ferreiros, D. Bon, et al., Variations in serum sphingolipid levels associate with liver fibrosis progression and poor treatment outcome in hepatitis C virus but not hepatitis B virus infection, Hepatology 61 (2015) 812–822.
[31] P.C. Schulze, K. Drosatos, I.J. Goldberg, Lipid use and misuse by the heart, Circ. Res. 118 (2016) 1736–1751.
[32] E. Gulbins, M. Palmada, M. Reichel, et al., Acid sphingomyelinase-ceramide system mediates effects of antidepressant drugs, Nat. Med. 19 (2013) 934–938.
[33] R. Dhami, X. He, E.H. Schuchman, Acid sphingomyelinase deficiency attenuates bleomycin-induced lung inflammation and fibrosis in mice, Cell. Physiol. Biochem. 26 (2010) 749–760.
[34] A. Moles, N. Tarrats, J.C. Fernandez-Checa, M. Mari, Cathepsin B overexpression due to acid sphingomyelinase ablation promotes liver fibrosis in Niemann-Pick disease, J. Biol. Chem. 287 (2012) 1178–1188.
[35] C. Li, R. Han, L. Kang, et al., Pirfenidone controls the feedback loop of the AT1R/p38 MAPK/renin-angiotensin system axis by regulating liver X receptor-alpha in myocardial infarction-induced cardiac fibrosis, Sci. Rep. 7 (2017) 40523.
[36] T. Yamane, A. Muramatsu, S. Yoshino, et al., mTOR inhibition by rapamycin increases ceramide synthesis by promoting transforming growth factor-beta1/Smad signaling in the skin, FEBS Open Bio 6 (2016) 317–325.

Please cite this article in press as: Y. Shi, et al., Sphingomyelin phosphodiesterase 1 (SMPD1) mediates the attenuation of myocardial infarction-induced cardiac fibrosis by astaxanthin, Biochemical and Biophysical Research Communications (2018), https://doi.org/10.1016/j.bbrc.2018.06.054